We are IntechOpen, the world's leading publisher of Open Access books
Built by scientists, for scientists

6,900
Open access books available

185,000
International authors and editors

200M
Downloads

154
Countries delivered to

Our authors are among the

TOP 1%
most cited scientists

12.2%
Contributors from top 500 universities

CLARIVATE ANALYTICS
BOOK CITATION INDEX
INDEXED

WEB OF SCIENCE™

Selection of our books indexed in the Book Citation Index
in Web of Science™ Core Collection (BKCI)

Interested in publishing with us?
Contact book.department@intechopen.com

Numbers displayed above are based on latest data collected.
For more information visit www.intechopen.com

Bulk High-Temperature Superconductors: Simulation of Electromagnetic Properties

Ekaterina Kurbatova, Pavel Kurbatov and Mikhail Sysoev

Abstract

The chapter deals with the electromagnetic properties of bulk high-temperature superconductors (HTSs), which can be used in magnetic systems for various applications, in particular, in contactless magnetic suspensions. Magnetic levitation in HTS material has a different nature from permanent magnets. It is caused by induced superconducting currents inside the volume of material. Due to this, the levitation is self-stabilizing and does not require additional active control or mechanical stops in magnetic systems with HTS. HTS materials have nonlinear, anisotropic, hysteresis properties, which make the calculation of the superconducting devices very difficult. Here you can find a brief overview of existing approaches to modeling HTS materials by E-J characteristics. Authors propose the method of simulation intending for 3D numerical calculation, which represents the processes in HTS using two types of magnetic field sources – current and magnetization. The chapter focuses on the analysis of sources inside the superconducting material and their influence on an external magnetic field and levitation properties of HTS. In addition to simulations, the experimental studies of the force interactions between HTS bulks and permanent magnet are presented and compared with the calculations to verify the proposed mathematical models.

Keywords: high-temperature superconducting, model of HTS, bulk superconductor, the Meissner effect, simulation, numerical calculation, magnetic field, magnetic levitation

1. Introduction

Using bulk high-temperature superconductors (HTSs) is caused by the peculiarity of their electromagnetic properties. Due to the low resistivity, which is almost zero in the superconducting state, induced currents in HTS practically do not fade and reach significantly higher values than the conventional conductive materials.

According to Faraday's law, the induced superconducting currents prevent the change in the magnetic field; therefore, after the transition into the superconducting state, HTS traps and saves the magnetic field in which they were cooled. Based on this feature, it is possible to create full magnetic levitation

characterized by self-stabilization in the directions of several degrees of freedom simultaneously. Unlike the passive magnetic bearing, where the interaction between permanent magnets provides the force, HTS suspensions do not require the additional active control or mechanical stops.

Most often, the schemes with the interaction of permanent magnets and bulk superconductors are used. In such constructions, two modes of HTS cooling are possible – zero-field cooling (ZFC) without external magnetic field and field cooling (FC) under the influence of the external field. In FC mode, HTS is cooled inside the magnetic system in the position that must be maintained. In this case, the HTS suspension is stable for any displacements. ZFC shows larger values of forces. However, it may lead to the instability of the system.

Creating of superconducting bearings [1–8], transportation systems (MagLev) [9–14], and other devices with HTS bulks requires the use of numerical calculation methods and specialized mathematical model describing their electromagnetic properties. Simulation of HTS bulks is a complex problem due to the necessity to consider the influence of nonlinear properties of superconducting material at work in magnetic fields and their interaction with the magnetic system.

In general, the following phenomena should be considered when modeling bulk HTS:

- transferring between the superconducting and the normal states;

- nonlinear resistance;

- the Meissner effect (exclusion of the field during cooling);

- trapping of a magnetic field;

- anisotropy; and

- hysteresis.

In this chapter, we briefly overview the existing models of HTS and present the method for simulation, which allows taking into account the various aspects of the bulk HTS properties listed above.

The possibilities of the proposed models are shown on simulation examples and compared with the experimental measurements. An example of a simulation of the magnetization process illustrates the distribution of magnetic field sources inside a superconductor. The behavior of HTS at different cooling modes, including the trapping of the magnetic field and the Meissner effect, is explained based on the analysis of simulation results.

The verification of the proposed method of simulation is performed by the comparison with measurements. Here we present the experimental study of the levitation force between a permanent magnet and HTS bulks, which is the most important in terms of the use of HTS bulks in magnetic suspensions and other levitation systems.

2. E-J characteristics of HTS

As a type of conductive material with a nonlinear resistivity, HTS is usually simulated by the E-J characteristics. The simplest model for the calculation of superconductors is *Critical State Model* [15–18]: when

$$\begin{cases} \mathbf{J} = J_C \dfrac{\mathbf{E}}{|\mathbf{E}|}, & when \ |\mathbf{E}| \neq 0 \\[2mm] \dfrac{\partial \mathbf{J}}{\partial t} = 0, & when \ |\mathbf{E}| = 0 \end{cases} \tag{1}$$

where $\mathbf{J}$ is the current density vector, $\mathbf{E}$ is the vector of the electric field strength, and J_C is the critical value of current density.

In this model, HTS is characterized by the E-J dependence at which the current in a superconductor cannot exceed a certain critical value J_C, and as the value of J_C is not achieved, the electric field is equal to zero (**Figure 1(a)**).

Determination of the critical current is an important problem in the simulation of HTS. The most common approaches are the Bean [15] and Kim [16] models. The Bean model assumes that J_C = *const*, and it is determined only by the properties of the superconductor. The studies in this area showed that J_C depends on external factors, in particular on the magnetic field. Thereby, the Kim model describes this influence as follows:

$$J_C = J_{C0} \frac{B_0}{B_0 + B}, \tag{2}$$

where B is the magnetic flux density, and J_{C0} and B_0 are the constants determined by the properties of a material. In general, J_{C0} and B_0 also depend on the temperature.

Extended Critical State Model [19, 20] was proposed to take into account the appearance of resistivity in case of exceeding J_C, caused by flux motion. This process can be modeled as a transition of a superconductor in the normal state (**Figure 1(b)**). For this purpose, the behavior of the superconductor in the flux-flow region [21, 22], when $J > J_C$, is defined using the additional equation:

$$E = \rho_f (J - J_C), \tag{3}$$

where ρ_f is the effective electrical resistivity. Thus, in this model, there are two areas, or conditions, in which the superconductor can be:
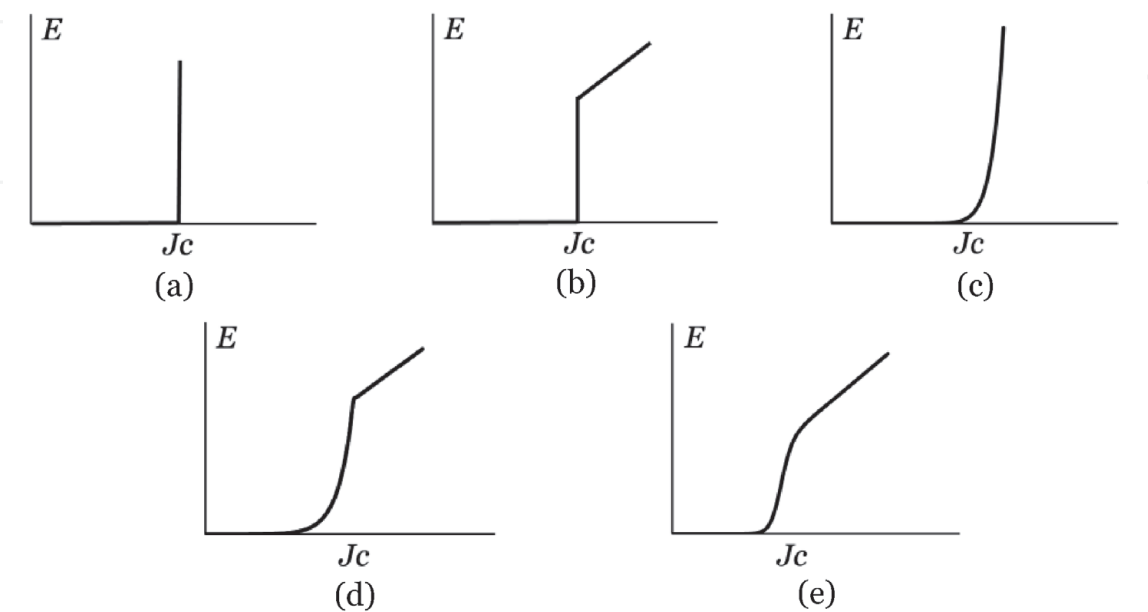

Figure 1.
E-J characteristics of HTS: (a) critical state model; (b) extended critical state model; (c) power law;
(d) flux-flow and flux-creep model; and (e) hyperbolic model.

$|J - J_C| < J_C$ – superconducting state corresponding to the critical state model and $J > J_C$ – appearance of the resistance caused by flux motion.

Critical current density and the effective electrical resistivity are the functions of the magnetic field strength:

$$J_C = J_0 \left(H_j/H\right)^n, \tag{4}$$

$$\rho_f = \rho_0 (H/H_{C2})^m, \tag{5}$$

where J_0 and H_j are the constants determined by the properties of material, ρ_0 is the resistivity of the superconductor in the normal state, and H_{C2} is the value of the second critical field.

The critical state model and its extension described above use linear approximation. This is an idealized representation of HTS properties. The real E-J dependence has nonlinear form, due to inhomogeneity of material and physical processes associated with the creep of fluxes, occurring with the increase of current. Such kind of dependence can be described using the *Power Law Model* [23, 24], which is a smooth approximation of the critical state model as shown in **Figure 1(c)**:

$$E = E_C \left(\frac{J}{J_C}\right)^n, \tag{6}$$

where E_C is the critical electric field strength, and n is the power law exponent that mainly influences the simulating properties [25].

Similar to J_C (Eq. (2)), n value depends on the magnetic field:

$$n = n_{C0} \frac{B_0}{B_0 + B}, \tag{7}$$

where n_{C0} and B_0 are the constants determined by the properties of material.

The power law model is the most commonly used for numerical calculations of superconducting materials. However, experimental determination of n value causes difficulties for HTS bulks [26].

One of the models that most accurately and completely describe the behavior of HTS is *Flux-Flow and Flux-Creep Model* [27, 28]. It divides the different types of conductivity in a high-temperature superconductor (**Figure 1(d)**):

$$E = \begin{cases} E_C \dfrac{\sinh\left(\beta J/J_C\right)}{\sinh(\beta)}, & when \quad J \leq J_C \\ E_C + \rho_{ff}(J - J_C), & when \quad J > J_C \end{cases}, \tag{8}$$

where ρ_{ff} is the flux-flow resistivity, parameter β characterizes the pinning:

$$\beta = U_0/k_B T, \tag{9}$$

where U_0 is the pinning potential, k_B is the Boltzmann constant, and T is the temperature.

When $J \leq J_C$, a superconductor is in the flux-creep region [29]. When $J > J_C$, both flux-creep and flux-flow [21, 22] effects are present in material simultaneously.

The critical current density in Eq. (8) depends on the magnetic induction according to the Kim model mentioned above. And the flux-flow resistivity is defined from the Bardeen-Stephan model

$$\rho_{ff} = \rho_{f0} \frac{B}{B_\rho}, \qquad (10)$$

where ρ_{f0} and B_ρ are the constants at a given temperature.

In some works, the electrical resistivity is represented as an approximating *Hyperbolic function* of magnetic field strength H, current density J, and temperature T [30, 31]:

$$\rho = 0.5\rho_0 \times \{1 + \text{th}[-(1 - T/T_C)(1 - H/H_C)(1 - J/J_C)/\delta_j]\}, \qquad (11)$$

where ρ_0 is the electrical resistivity of the HTS material in the normal states (constant); J_C is the critical current density; H_C is the critical magnetic field strength; T_C is the critical temperature; and δ_j is the relative dispersion of the distribution of critical parameters in the inhomogeneous material.

E-J characteristic corresponding to Eq. (11) is shown in **Figure 1(e)**. This approximation is similar to the flux-flow and flux-creep model and allows to describe the properties of HTS in different regions.

For this model, the dependence of the critical current density on the magnetic field strength is determined by the power functions:

$$\begin{cases} J_C = \pm J_{C,\max} \cdot (1 - (H/H_c)^\alpha)^\beta, & when \quad H \leq H_C \\ J_C = 0, & when \quad H > H_C \end{cases}, \qquad (12)$$

or

$$J_C = \pm J_{C,\max} / (1 + (H/H_c)^\alpha)^\beta, \qquad (13)$$

where $J_{C,\max}$ is the maximum value of the critical current density at a given temperature, and α and β are the model parameters (real positive numbers). Variation of α and β allows us to change the form of the $J_c(H)$ dependence in a wide range. The maximum value of the critical current density is defined by the following temperature dependence:

$$J_{C,\max} = J_{C0}\left(1 - (T/T_C)^2\right)^n, \qquad (14)$$

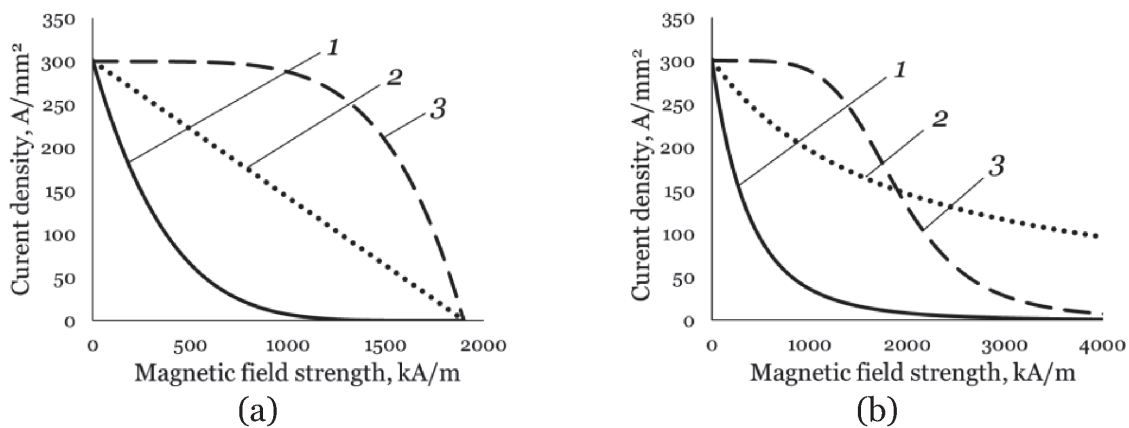$$H_C = H_{C0}\left(1 - (T/T_C)^2\right)^m, \qquad (15)$$

Figure 2.
Dependencies of the critical current density on the magnetic field strength at a constant temperature: (a) according to Eq. (12) and (b) according to Eq. (13). 1 – α = 1, β = 5; 2 – α = 1, β = 1; and 3 – α = 5, β = 1.

where J_{C0} and H_{C0} are the critical current density and critical magnetic field strength extrapolated to $T = 0$; Tc is the critical temperature, at which superconductivity is lost; and n and m are the positive real numbers.

Figure 2 illustrates the dependencies of the critical current density on the magnetic field strength at a constant temperature, according to Eqs. (12) and (13) with different coefficients α and β and the following critical parameters: $J_{C,\max}$ = 300 kA/mm^2 and H_C = 2000 kA/m.

3. Method for simulation of HTS

The manufacturing technology of high-temperature superconducting materials determines their structure and electromagnetic properties. In general, mathematical models of the properties of such materials should describe not only the flow of conductivity currents, so-called "transport currents," but also the possible existence of small volume-distributed regions having magnetic properties similar to a nonlinear diamagnetic material. These regions can be represented as isolated superconducting regions in which circulating currents interact with the magnetic field according to a certain law as microcurrents in magnetic materials.

For numerical calculations, the distribution of superconducting currents can be approximated by the complex current vector models with two basic components: the transport current density **J** and the magnetization **M**. To analyze an electromagnetic field, the sources **J** and **M** are represented in a volume of HTS by continuous functions of magnetic field parameters, that is, averaged at a macroscopic level.

The transport current **J** is induced to oppose the applied field in accordance with Faraday's law [32], which can be written for **J** using the relation **E** = ρ**J**

$$\mathbf{J} = -\frac{1}{\rho}\left(\frac{d\mathbf{A}}{dt} + \nabla\varphi\right), \tag{16}$$

where ρ is the electrical resistivity as the function of the magnetic field strength H, current density J, and temperature T. The electrical resistivity in superconductors is usually anisotropic and is represented by the resistivity tensor. Here we use the hyperbolic function Eq. (11), which describes the properties of HTS in a wide range and has functional customization. However, for the region without flux-flow resistance, the power law (Eq. (6)) will show similar results.

The vector magnetic potential **A** is the time-dependent function of magnetic field sources **J** and **M**

$$A(t) = \frac{\mu_0}{4\pi}\left[\int_V \frac{\mathbf{J}(t) + \nabla \times \mathbf{M}(t)}{r}dV - \oint_S \frac{\mathbf{n} \times \mathbf{M}(t)}{r}dS\right] + \mathbf{A}^{\text{ext}}(t), \tag{17}$$

where **A**$^{\text{ext}}$ is the vector potential created by the external sources.

The scalar electric potential φ determines the potential component of the electric field strength

$$\mathbf{E}^p = -\nabla\varphi = -\frac{1}{4\pi\varepsilon_0}\oint_S \frac{\xi(t)\mathbf{r}}{r^3}dS + \mathbf{E}^{p,\text{ext}}, \tag{18}$$

where ξ is the density of the electric charges induced on the surface of a super-conductor, and $\mathbf{E}^{p,ext}$ is the electric field strength created by the external sources. The electric charge density is determined using the integral boundary equations.

Detailed information about Eqs. (17) and (18) can be found in Ref. [32].

The magnetization is determined from the stationary state equations and properties of material

$$\begin{cases} \mathbf{B} = \nabla \times \mathbf{A} \\ \mathbf{B} = \mu_0 (\mathbf{H} + \mathbf{M}) \end{cases}. \tag{19}$$

Magnetization is associated with another type of source-related currents circulating in the isolated regions as mentioned above. These currents have the same properties as transport current in terms of depending on the temperature and magnetic field strength but have the form of small local vortex structures with the magnetic moment vectors **m.** For modeling the contribution of these local currents, they can be represented as the distribution of superconducting solenoids, which length is much more than its diameter.

If we consider such long solenoid, the intrinsic magnetic field strength inside it is close to uniform and equal to the linear current density. Thus, it is assumed that the local current structures are equivalent to uniformly magnetized elements along the axis. The own demagnetizing magnetic field strength of the solenoid is zero.

As a parameter of the material properties, the magnetization M is the density of magnetic moments of the superconducting solenoids [33]. Until the magnetization M in a superconductor is less than the value of the critical magnetization Mc, the magnetic flux density inside the superconducting solenoids remains constant and equal to the previously acquired value. It means that in the region $M < Mc$, the magnetization is changed according to the equation for a diamagnetic material

$$\frac{dM}{dH} = -1. \tag{20}$$

Due to the relation with the superconducting currents, the critical magnetization is characterized by the nonlinear dependence on the magnetic field like in Eqs. (12) and (13)

$$\begin{cases} M_C = \pm M_{C,\max} \cdot (1 - (H/H_{CM})^\alpha)^\beta, & when \quad H \leq H_{CM} \\ M_C = 0, & when \quad H > H_{CM} \end{cases}, \tag{21}$$

or

$$M_C = \pm M_{C,\max} / (1 + (H/H_{CM})^\alpha)^\beta, \tag{22}$$

where $M_{C,\max}$ is the maximum value of critical magnetization at a given temperature, and H_{CM} is the critical magnetic field strength for magnetization. The temperature dependencies of the critical magnetization and critical magnetic field strength are the same as for the hyperbolic model in Eqs. (13) and (14).

The model parameters α and β for the magnetization may differ from their values in the equations for the current density. **Figure 3** presents the dependencies of the maximum critical magnetization at a constant temperature according to Eqs. (21) and (22) with different coefficients α and β and the following critical parameters: $M_{C,\max}$ = 500 kA/m and H_{CM} = 2000 kA/m.

Figure 4 shows the magnetization curve of a superconductor obtained using Eqs. (20) and (21). If HTS has been transferred into the superconducting state without an external magnetic field (ZFC), then the magnetization in the initial state is zero (point 0). With increasing magnetic field strength, the magnetization increases in the opposite direction to satisfy the condition of an ideal diamagnetic $M = -H$ (magnetic induction inside the diamagnetic equals zero) until point 1. From this point, the magnetization is limited by the critical curve $M_C = f\,(H)$ up to $M_C = 0$ at point 6. Changing the magnetic field in the range $-M_C < H < M_C$ does not cause the trapping of a magnetic field, and magnetization is defined by the linear region of the characteristic. If the magnetic field strength decreases from the point on the critical line (point 2), then the magnetization will be defined from the condition of the constant value of magnetic induction B_2 as $M = B_2/\mu 0 - H$, where B_2 is the value of magnetic flux density at point 2. At point 3, the magnetization reaches the critical value on the upper part of the magnetization curve, and further-more, it will be determined by the critical curve $M_C = f\,(H)$ up to point 7. If the magnetic field decreases at point 4, the new value of magnetic induction B_4 will remain constant until the critical magnetization at point 5. At field cooling (FC), the magnetization changes similarly, but the initial point is determined by the magnetic field $H \neq 0$ either on the initial line 0–1 or on the critical curve 1–6.
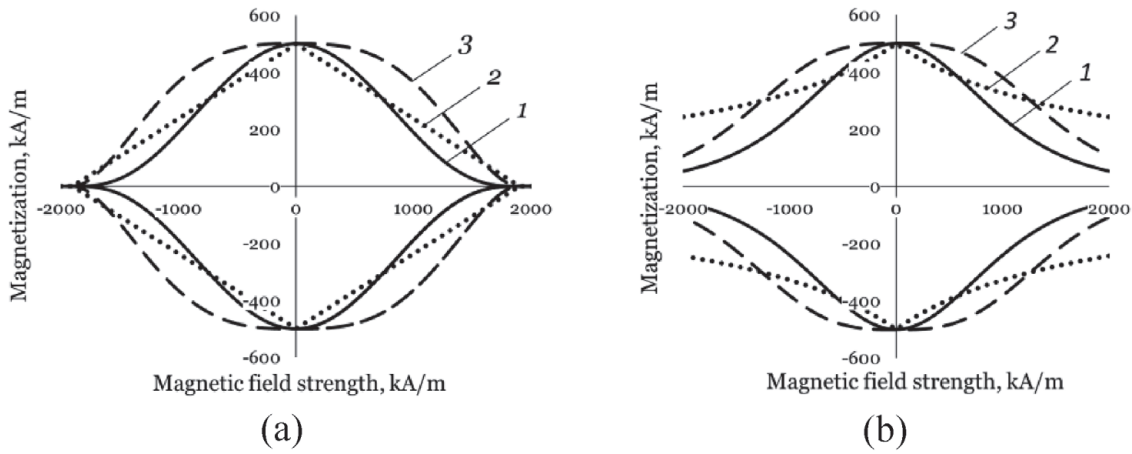

Figure 3.
Dependencies of the maximum critical current density on the magnetic field strength at a constant temperature: (a) according to Eq. (21) and (b) according to Eq. (22). 1 – α = 2, β = 3; 2 – α = 1, β = 1; and 3 – α = 3, β = 2.
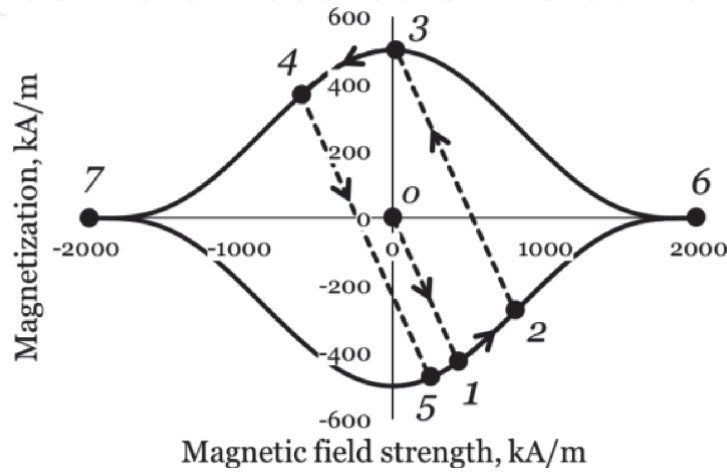

Figure 4.
Changing the magnetization under variation of a magnetic field (magnetization curve of HTS).

We assume that in a certain small volume of the superconductor, there are a sufficiently large number of solenoids, which may have different parameters of the critical magnetization dependencies. Inhomogeneity of the magnetization properties is taken into account using the probabilistic distribution laws for the mentioned parameters. **Figure 5** presents the comparison of the volume-averaged magnetization determined for a superconducting material with homogeneity and inhomogeneity properties. In the first case, all superconducting solenoids are identical. In the second case, solenoids have different critical parameters and, accordingly, create different magnetic moments.

The spatial orientation of the solenoids defines the anisotropic properties of the magnetization. $M(H)$ characteristics in **Figure 5** represent the properties along the axis of the solenoids, which have identical directions in a volume of superconductor. The orthogonal components of the magnetic field strength do not create magnetization. This corresponds to the usually used assumption that currents flow in the plane perpendicular to the anisotropy axis.

In general case, the anisotropic properties can be simulated using the probability distribution of both the values of critical parameters and directions. **Figure 6** shows an example of the dependence of the magnetization along the main axis of anisotropy α as a function of the components of the magnetic field strength along the axes α and β.

The idea of combining the models for current and for magnetization in the simulation of HTS bulks is as follows. Applying the external magnetic field after
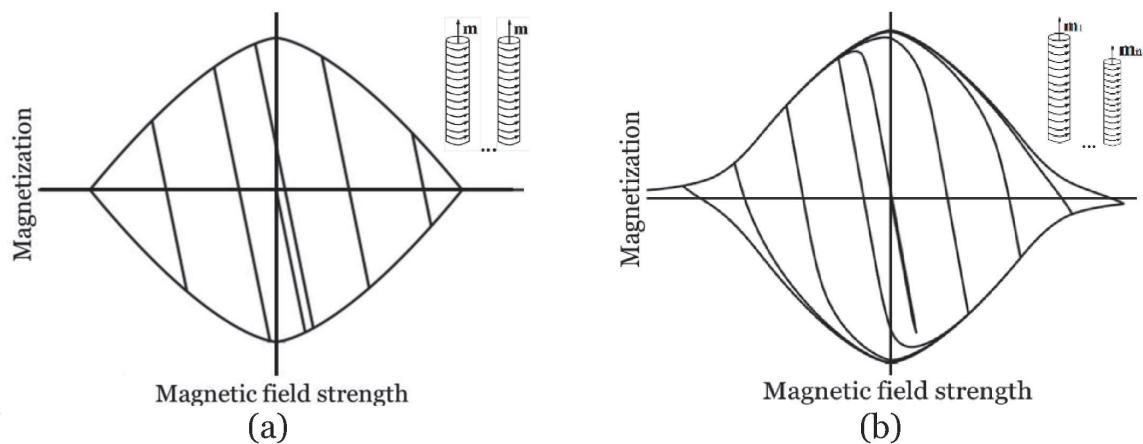

Figure 5.
Magnetization curve of HTS bulk with homogeneity (a) and inhomogeneity (b) properties.
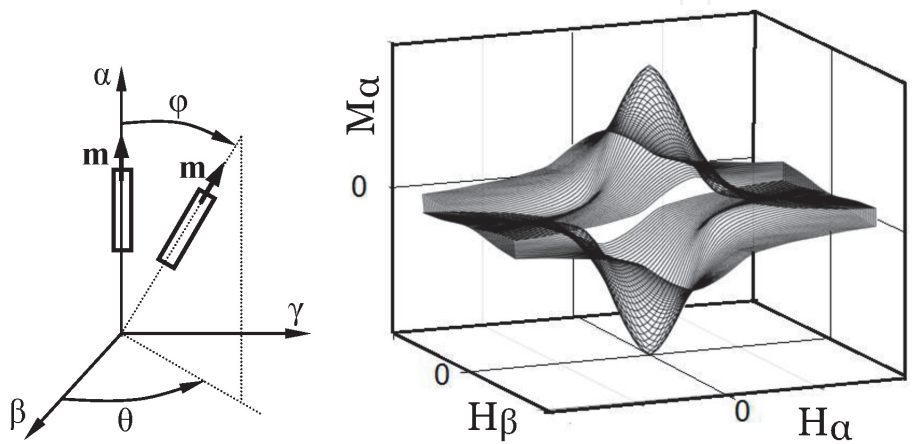

Figure 6.
Magnetization model with anisotropy.

cooling the superconductor at ZFC mode leads to the appearance of the induced transport currents. These currents are defined by both the external magnetic field and the own magnetic field of superconductor created by the resulting magnetization and induced currents. During the cooling process at FC mode, the magnetization occurs to expel the magnetic field from the volume of HTS as in type I superconductors. Changes of the resulting magnetic field due to the magnetization causes induced currents to flow according to Faraday's law. In this case, currents and magnetization create magnetic fields that try to compensate for the influence of each other. If the compensation of magnetic fields does not full, there will be the partial exclusion of the magnetic field from the superconductor. Thus, it is possible to simulate the partial Meissner effect at FC mode.

4. Simulation of J and M sources in HTS bulk

This section presents the analysis of the distribution of field sources in a bulk high-temperature superconductor. Computational model for analyzing the interaction of HTS bulk with the external magnetic field, which is shown in **Figure 7**, illustrates the simulation of superconductor using the proposed mathematical models for two types of electromagnetic field sources *J* and *M*. In this example, superconducting disk 1 is placed in the magnetic field created by the DC coil 2. Changing the current in the coil provides two different types of transferring HTS disk into the superconducting state: zero-field cooling (ZFC) in the absence of a magnetic field and field cooling (FC) in the presence of a magnetic field.

MMF in the coil is set as a time function (**Figure 7(c)**) depending on the cooling mode. In ZFC, the calculation starts with zero MMF, after which the current linearly increases until the maximum value and then goes back to zero. In FC, the initial MMF is equal to the maximum value. It remains constant for 1 s and then decreases to zero. This delay does not affect the simulation and had been used only for the convenience of comparison between calculated results at ZFC and FC modes.

The process of magnetizing the HTS disk allows us to analyze the behavior of different sources, including the features of distribution inside the volume of superconductor and their influence on the magnetic field near the disk. Here, we carried out the calculations with three different models of HTS properties: model only for current, model only for magnetization, and combined model with current and magnetization. Despite the fact that both magnetization and current describe the motion of charges inside an HTS, that is, superconducting currents, as mathematical models of magnetic field sources, they have different properties and obey
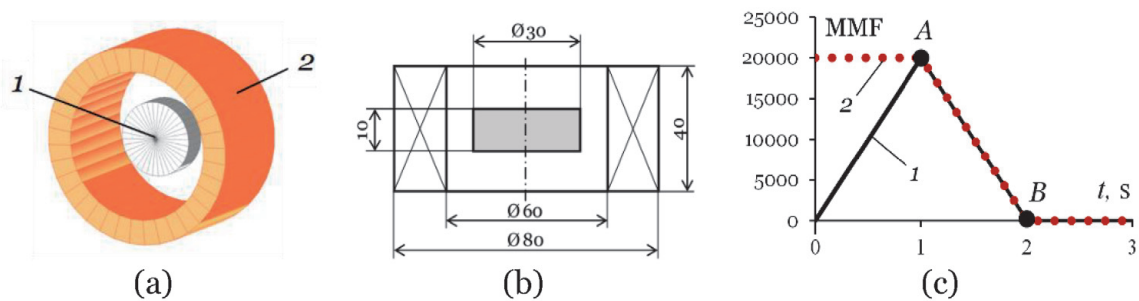

Figure 7.
Computational model for analysis of the interaction HTS bulk with the external magnetic field: (a) 3D model for calculation: 1 – HTS disk, 2 – field coil; (b) dimensions of the elements; and (c) MMF in the coil: 1 – ZFC, 2 – FC.

different laws. This causes relevant differences in the magnetizing process, as shown below.

Parameters of the mathematical model for M and J used for simulation in this section are given in **Table 1**. Temperature is assumed to be a constant value of 77 K, and the critical temperature is 93 K.

Figure 8 presents the distribution of magnetic field sources in a section of HTS disk in the case of ZFC. Results are presented for two specific time points: point A – at the maximum value of MMF ($t = 1.0$ s) and point B – at zero MMF ($t = 2.0$ s). The current density was calculated using the model only for the current density (Eqs. (11) and (12)); the magnetization was obtained from the calculation with the model only for the magnetization (Eqs. (20) and (21)).

Parameter	Units	Value
Critical current density, $J_{C,\max}$	A/mm^2	300
Critical magnetic field for current, H_C	kA/m	2300
α for critical current	—	1
β for critical current	—	2
Dispersion δ	—	0.01
Critical magnetization, $M_{C,\max}$	kA/m	1000
Critical magnetic field for magnetization, H_{CM}	kA/m	2300
α for magnetization	—	1
β for magnetization	—	2

Table 1.
*Parameters of the mathematical models for J and M used in simulation in **Figure 7**.*

Model for current   Model for magnetization

$t_A = 1.0$ s

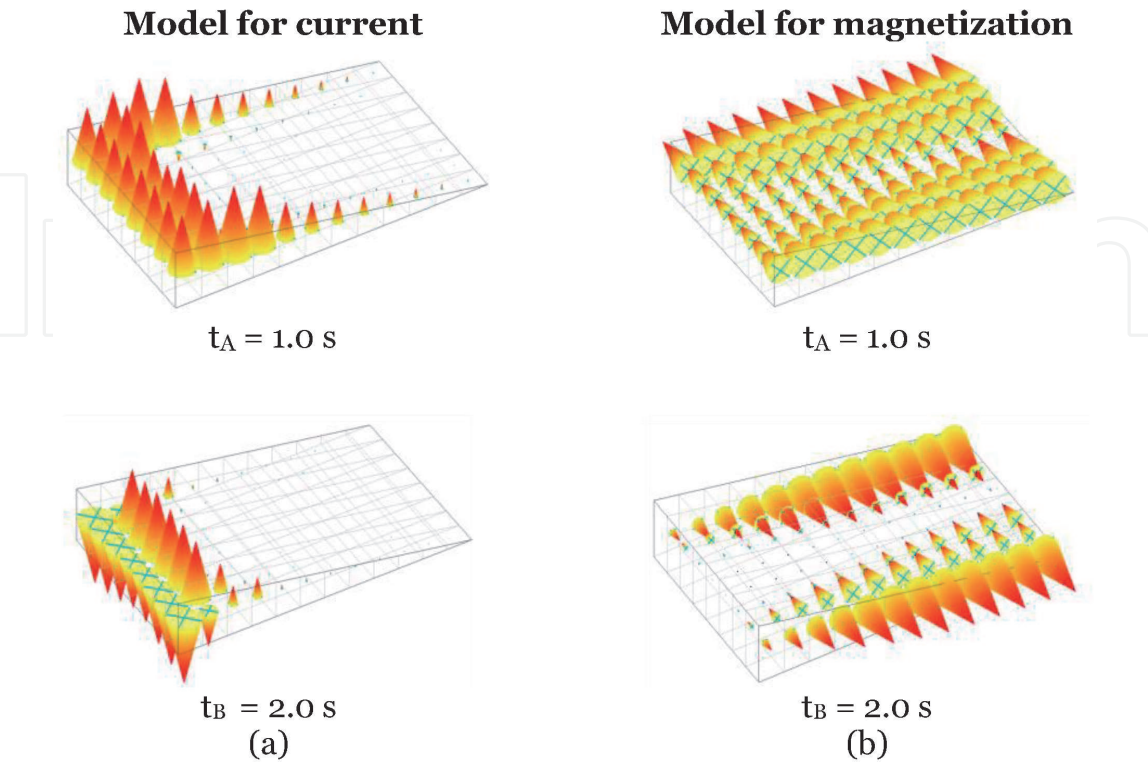$t_A = 1.0$ s

$t_B = 2.0$ s

$t_B = 2.0$ s

(a)

(b)

Figure 8.
Distribution of the magnetic field sources in a section of the HTS disk at ZFC: (a) model for current and (b) model for magnetization.

After transferring into the superconducting state, HTS prevents the change of the magnetic field inside its volume. At point A, current and magnetization try to compensate the magnetic field of the coil. However, due to the nonlinear properties of HTS, exceeding a certain value of the external field causes the magnetic field to penetrate inside the superconductor. Therefore, even after ending the current impulse at point B, both magnetic field sources save the trapped magnetic field. The maximum value of the external magnetic field, which can be compensated by HTS bulk, depends on the critical parameters of the mathematical models (J_C and M_C).

Figure 9 shows the distribution of magnetic field sources inside HTS in the case of ZFC obtained from the calculation using the combined model at similar time points. In the combined model, both magnetic field sources exist simultaneously and affect each other.

The combined model reproduces the features of the magnetizing process after ZFC that is compensating and trapping the external magnetic field as well as conventional models for current. The impact of an additional field source in the form of magnetization leads to a change in the distribution of current density inside the volume of HTS compared with the results of the model only for current. Currents in **Figure 8** are induced on the side surface of the disk over the entire height and gradually penetrate the volume. In contrast, in the combined model, the magnetization vectors also take part in compensation of the magnetic field, and currents flow only on the end faces of the disk filling the volume of HTS from the outer radius. The induced currents also affect the distribution of magnetization, which differs from that shown in **Figure 8**. This is especially observed at point B when HTS traps a part of the external magnetic field.

Distribution of the magnetic field near HTS disk is defined by the type and localization of magnetic field sources. **Figure 10** presents the calculated distribution of the axial H_Z and radial $H\rho$ components of the magnetic field strength along the radius on a distance of 1 mm above the superconductor at ZFC. Dependences for three considered models of HTS properties are shown at two specific time points,
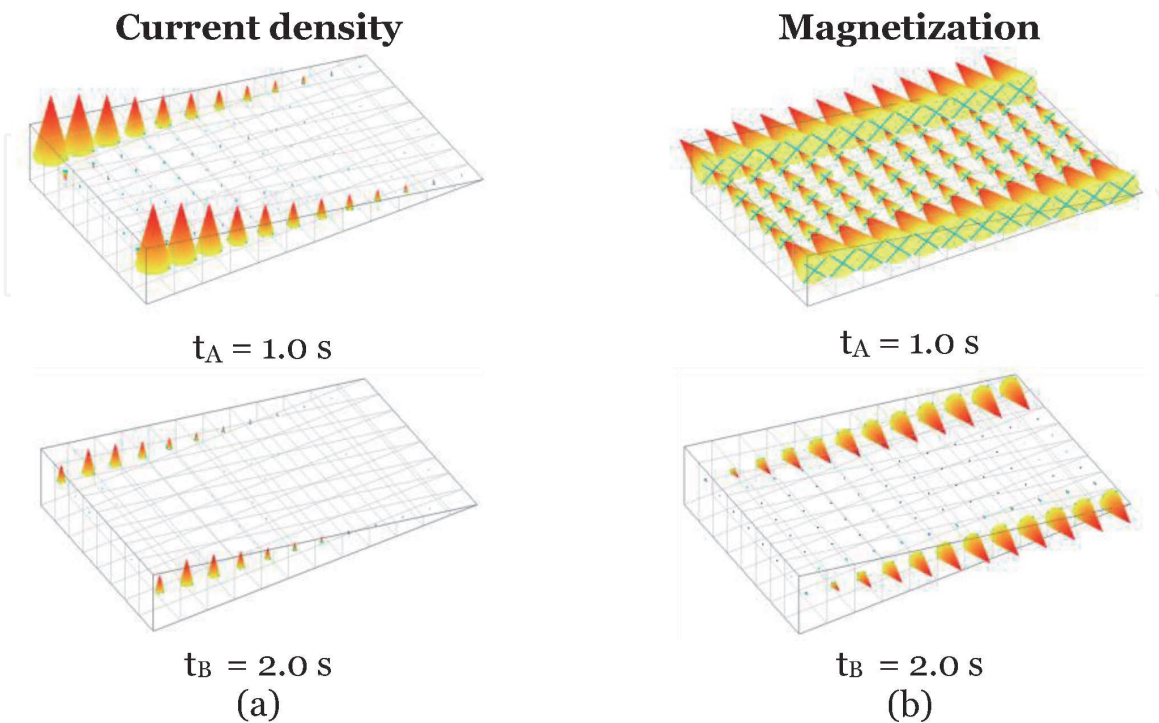

Current density   **Magnetization**

$t_A = 1.0$ s $t_A = 1.0$ s

$t_B = 2.0$ s $t_B = 2.0$ s

(a)   (b)

Figure 9.
Distribution of the magnetic field sources in a section of the HTS disk at ZFC using the combined model: (a) current density and (b) magnetization.
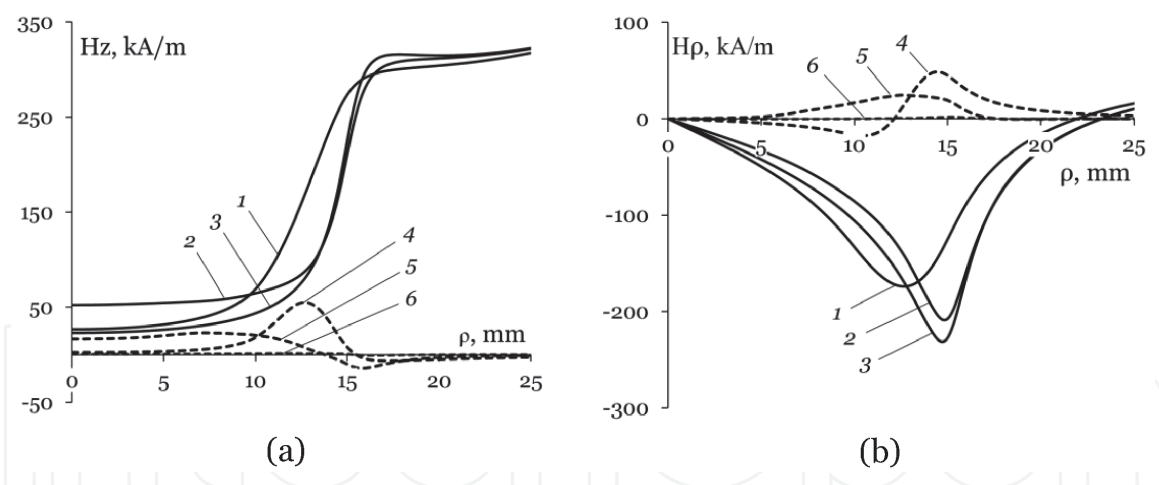
Figure 10.
Distribution of the axial (a) and radial (b) components of the magnetic field strength along the radius of HTS disk at ZFC: 1 – model for current at t_A = 1.0 s; 2 – model for magnetization at t_A = 1.0 s; 3 – combined model at t_A = 1.0 s; 4 – model for current at t_B = 2.0 s; 5 – model for magnetization at t_B = 2.0 s; and 6 – combined model at t_B = 2.0 s.

corresponding to above presented distributions of magnetic field sources: the maximum MMF (point A) – lines 1–3, and zero MMF (point B) – lines 4–6.

The obtained dependencies show that the model for magnetization gives a more uniform distribution of the axial component of the magnetic field strength than the model for current when the magnetic field penetrates HTS disk (point A). At the same time, the model for magnetization has a higher maximum and a sharper change of the radial component of the magnetic field strength at the border of HTS disk. At point B, the trapped magnetic field has a significant difference caused by the nature of the magnetic field created by currents and magnetization. A more pronounced difference is observed at point B because at this time, there is no external magnetic field, which primarily defines the distribution of the magnetic field at point A.

The distribution of the magnetic field strength for the combined model at point A is transitional between the results of calculations using the model only for current and the model only for magnetization. Thus, it becomes possible to customize the model of HTS properties by choosing model parameters and introducing weighting factors defining the contribution of each magnetic field source on the properties of superconducting material. The final condition of HTS is defined by the resulting influence of the current and magnetization and achieved when both sources come to a balance point, which is determined by the parameters of their models. In considered example with the applied model parameters, the magnetization almost completely compensates the impact of the induced current and its magnetic field. This leads to the absence of a trapped magnetic field at point B.

A similar simulation was carried out for cooling the HTS bulk in the magnetic field of DC coil. **Figure 11** presents the distribution of magnetic field sources in a section of a superconducting disk in the case of FC. Results are presented for two specific time points, similar to ZFC: point A – before changing the MMF (t = 1.0 s) and point B – at zero MMF (t = 2.0 s). The current density was calculated using the model only for the current density (Eqs. (11) and (12)); the magnetization was obtained from the calculation with the model only for the magnetization (Eqs. (20) and (21)).

When type I superconductor is cooled in an external magnetic field (FC), the magnetic field is excluded from its volume. This phenomenon is called the Meissner effect. In type II superconductors, this effect appears partially; therefore, usually it is not taken into account in calculations. As you can see in **Figure 11**, the current is
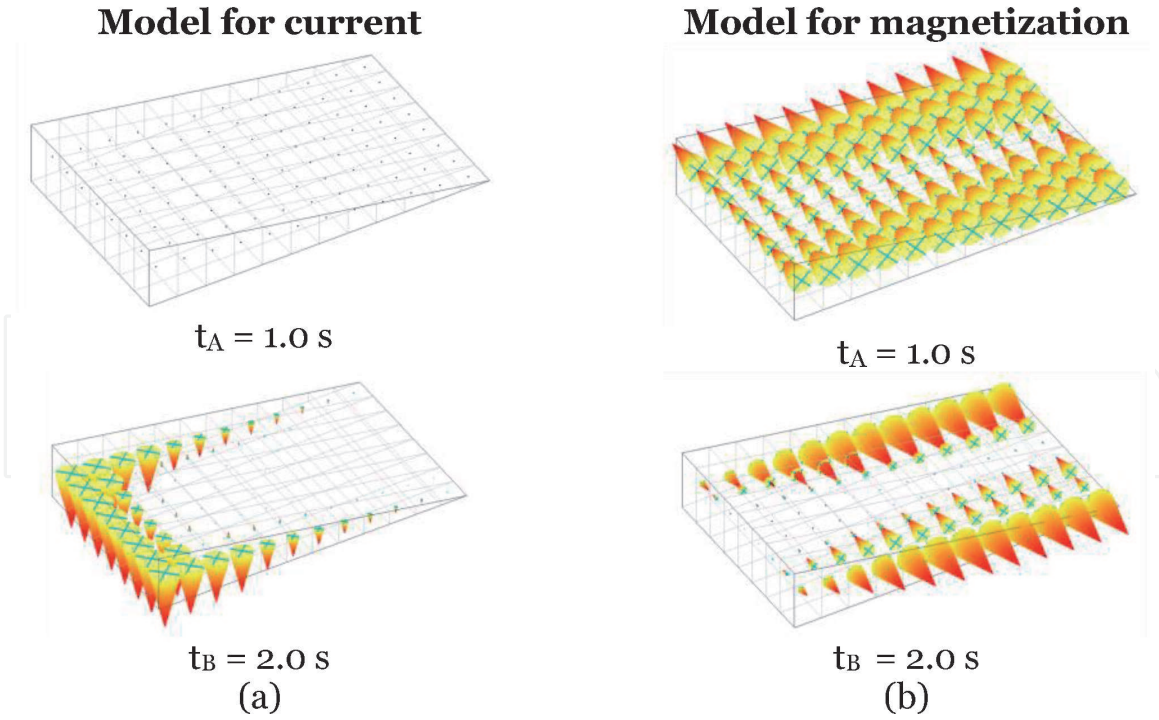
Figure 11.
Distribution of the magnetic field sources in a section of the HTS disk at FC: (a) model for current and (b) model for magnetization.

not induced at point A, since there is no change in the magnetic field during FC. In contrast to the model for current, the magnetization appears at the initial time and partially compensates the magnetic field inside the disk. However, due to the limitation of magnetization, most of the magnetic field penetrates the superconductor and then is trapped by it. At point B, both magnetic field sources are distributed in such a way as to trap the maximum of the magnetic field, which depends on the critical parameters of the mathematical models (J_C and M_C).

Figure 12 shows the distribution of the current density and magnetization vectors in a section of the HTS disk in the case of FC obtained from the calculation using the combined model with current density and magnetization at similar time points. Upon transition into the superconducting state, the magnetization and current appear simultaneously (point A). Magnetization provides the expulsion of the magnetic field from the volume of a superconductor (the partial Meissner effect). This causes a change in the magnetic field and inducing of superconducting current, which partially or wholly compensates the change of the magnetic induction in HTS. Therefore, unlike the model only for currents, when using the combined model, induced currents are observed even during FC. As for the trapped magnetic field at point B, it is provided by both sources, the distribution of which is similar to the separate mathematical models taking into account their influence on each other. Obtained distribution of currents and magnetization at FC mode for the combined model differs from the distributions of these sources in the ZFC mode. This mainly applies to currents, which occur on the side surface of the superconducting disk rather than on the end faces.

Figure 13 presents the calculated distribution of the axial H_Z and radial $H\rho$ components of the magnetic field strength along the radius on a distance of 1 mm above the superconductor at FC mode. Dependences for three considered models of HTS properties are shown at two specific time points, corresponding to the presented above distributions of magnetic field sources: before changing the MMF (point A) – lines 1–3 and at zero MMF (point B) – lines 4–6.
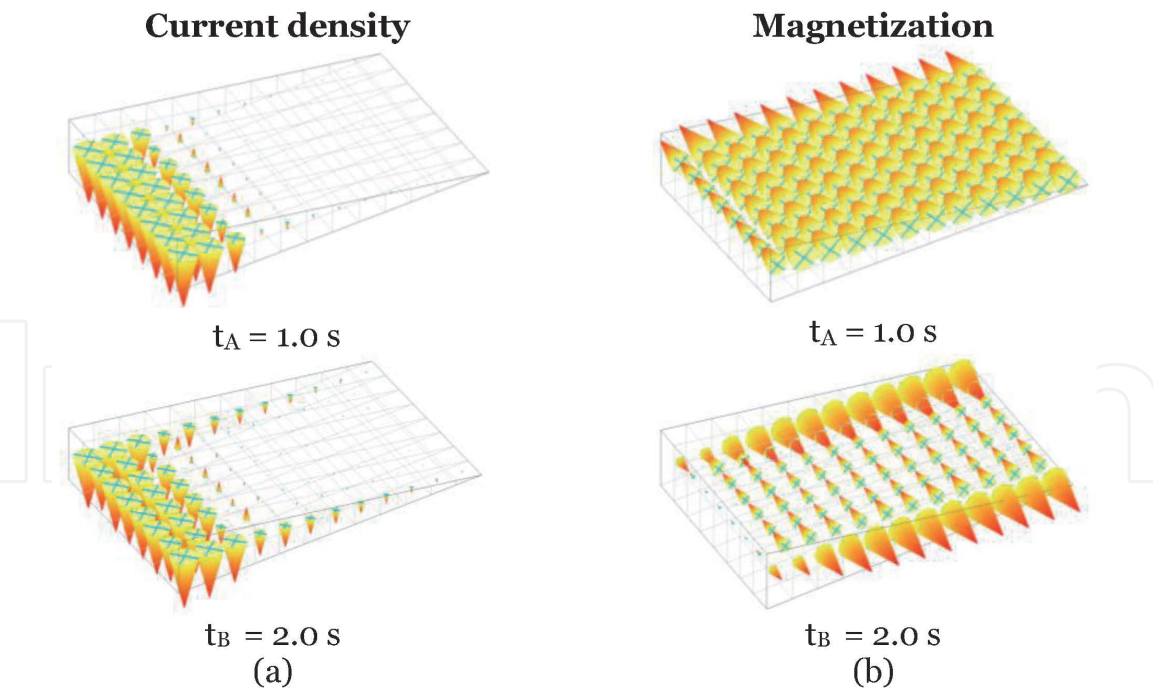
Figure 12.
Distribution of the magnetic field sources in a section of the HTS disk at FC using the combined model:
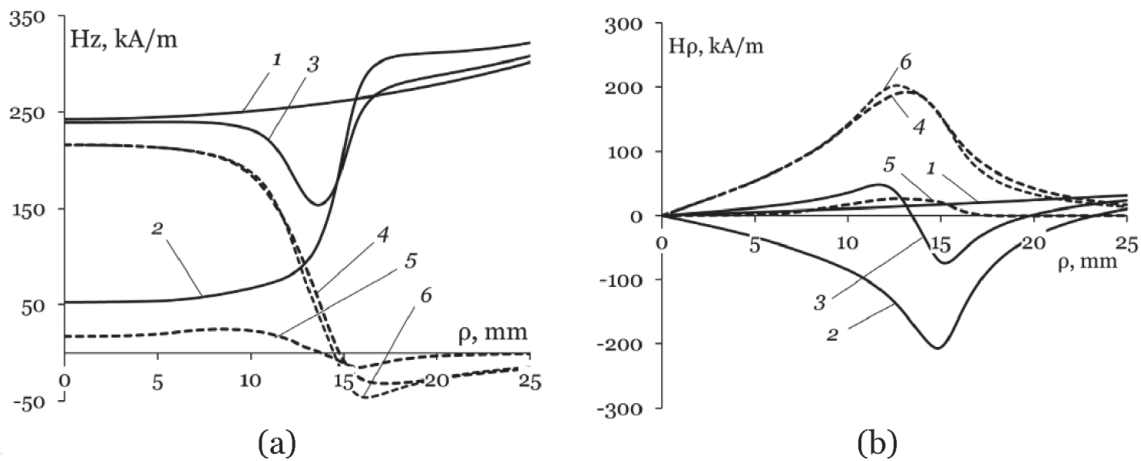*(a) current density and (b) magnetization.*

Figure 13.
Distribution of the axial (a) and radial (b) components of the magnetic field strength along the radius of HTS disk at FC: 1 — model for current at $t_A = 1.0$ s; 2 — model for magnetization at $t_A = 1.0$ s; 3 — combined model at $t_A = 1.0$ s; 4 — model for current at $t_B = 2.0$ s; 5 — model for magnetization at $t_B = 2.0$ s; and 6 — combined model at $t_B = 2.0$ s.

The obtained results of simulation indicate that the model for currents does not allow reproducing the Meissner effect in FC mode since the current in the HTS disk cannot be induced without changing the magnetic field. At point A, line 1 corresponds to the distribution of the magnetic field created by the current in the coil since the HTS disk does not affect it. In the model for magnetization, the resulting magnetic field due to the influence of magnetization significantly changes above the superconductor. Expulsion of the magnetic field from the volume of superconductor leads to a decrease in the axial component of the magnetic field strength and an increase in the radial component of the magnetic field strength compared with the coil field. The combined model shows the ability to control the nature of the source distribution and, accordingly, to adjust the Meissner effect and the redistribution of the magnetic field during FC mode quantitatively by choosing the model parameters.

At point B, the combined model and the model only for current show almost the same distribution of the trapped magnetic field. This is explained by the fact that the model for current mainly determines the trapped magnetic field in HTS at FC, while magnetization describes the changes of the magnetic field inside the superconducting material, which do not obey Faraday's law, including the Meissner effect.

5. Comparison with experimental measurements

Experimental study of the interaction force between a permanent magnet and HTS bulks, the so-called levitation force, was performed to provide data for the validation of the proposed mathematical models. Measurements were carried out on the laboratory equipment as shown in **Figure 14**.

Studied HTS sample 1 is placed and fixed inside the cuvette 2 using a nonmagnetic holder. For measuring the dependence of force on the gap between a permanent magnet and HTS, we use a moving rod 3, which is driven by a stepping motor. At the end of the rod, there is a fixed steel disk 4 holding the cylindrical permanent magnet 5 due to an attractive magnetic force. Weight 6 measures the force acting on the cuvette with HTS, and position sensor 7 shows the displacement of the permanent magnet during the experiment. Measuring equipment and a motor are connected to a computer that controls the experiment. For cooling, we used liquid nitrogen. Dimensions of the permanent magnet and two studied HTS samples (disk and ring) are shown in **Table 2**.

Force has been measured for two cooling modes: zero-field cooling and field cooling. During ZFC, the superconductor is cooled at the maximum gap of 50 mm. Then, the gap is installed at the initial measuring value of 29 mm. At FC, cooling process takes place at the gap of 3 mm. After cooling, the permanent magnet slowly moves vertically to or from HTS sample depending on the cooling mode.

Due to the properties of the high-temperature superconductors, the initial force curve differs from the subsequent ones. Therefore, the measurement along the
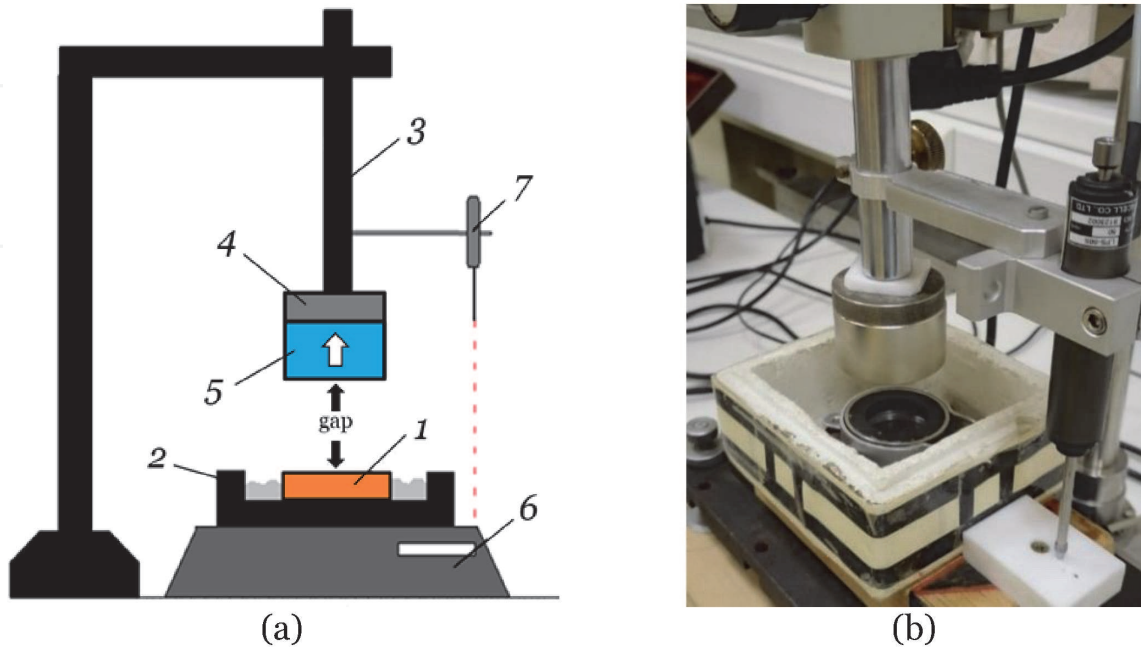

Figure 14.
Experimental measurements of the levitation force: (a) scheme of the experiment and (b) – photo of the laboratory equipment. 1 – HTS sample, 2 – cuvette, 3 – moving rod, 4 – steel disk, 5 – permanent magnet, 6 – weights, and 7 – position sensor.

	HTS disk	HTS ring	Permanent magnet
External diameter, mm	46	46	50
Inner diameter, mm	—	30	—
Height, mm	7	7	30

Table 2.
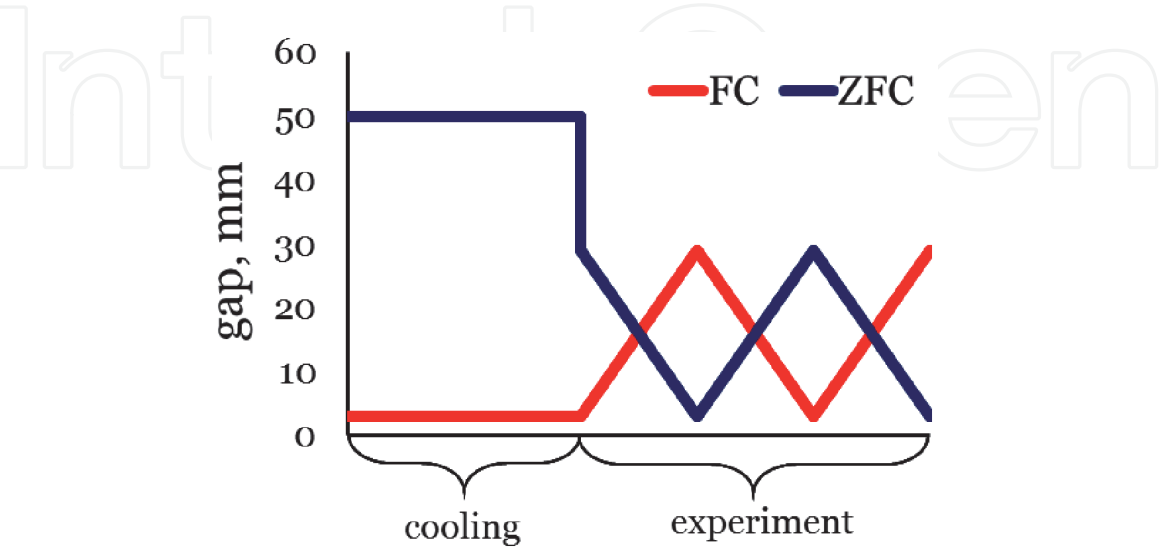*Dimensions of the permanent magnet and HTS samples.*

Figure 15.
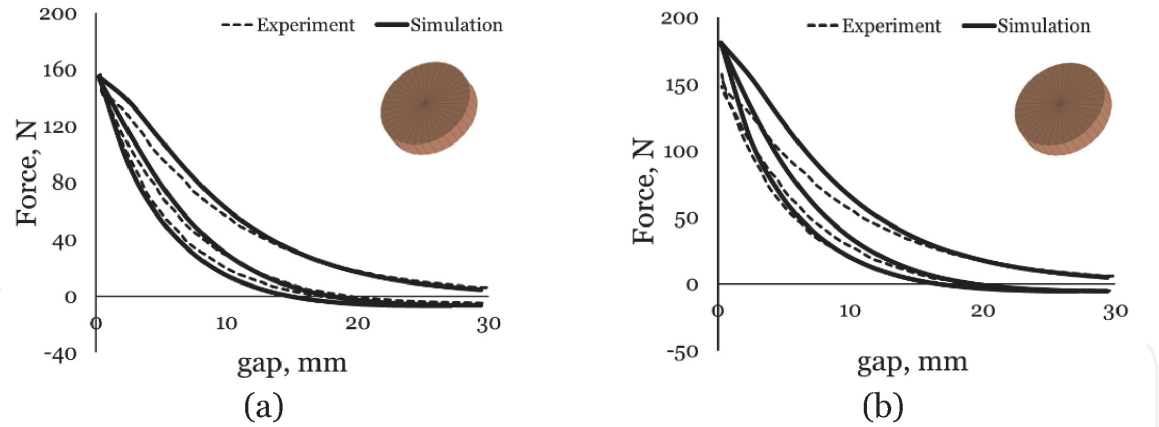*Changing the gap during the experiment for FC and ZFC.*

Figure 16.
Force of HTS disk for ZFC: (a) model for current and (b) combined model.

initial trajectory was performed twice to obtain stable characteristics. Thus, the change of the gap looks like this: 29–0.2–29–0.2 mm after ZFC and 3–29–3–29 mm after FC, as shown in **Figure 15**. With further cyclic loads, the obtained force dependencies will be repeated.

Experimental dependencies of the levitation force on the gap between the permanent magnet and HTS samples are compared with simulated results in **Figures 16–19**. The presented calculated characteristics have been obtained after selecting and optimizing the parameters of mathematical models described in Section 2 of this chapter.

Despite the fact that the approximation models have many parameters and due to this, they allow achieving excellent agreement with the experimental results in particular cases, defining the parameters is not an easy task on practice.
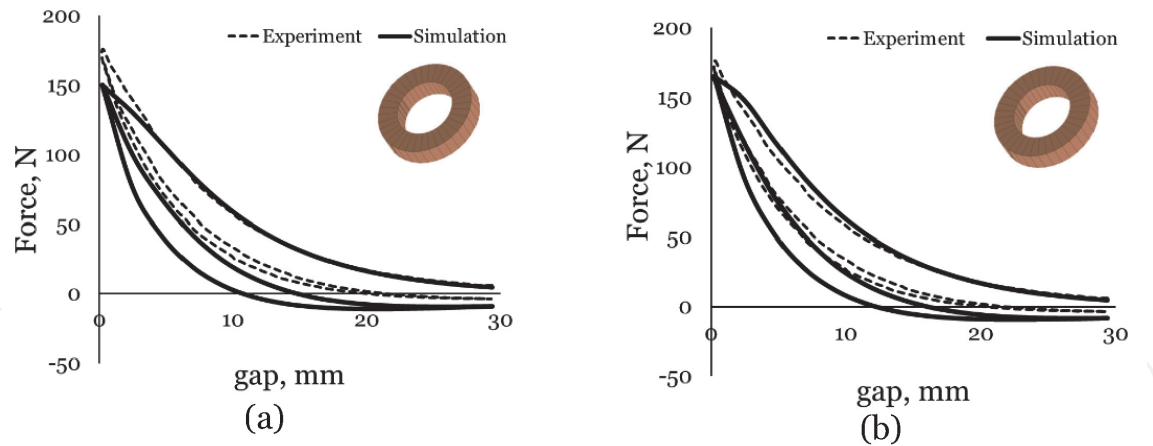
Figure 17.
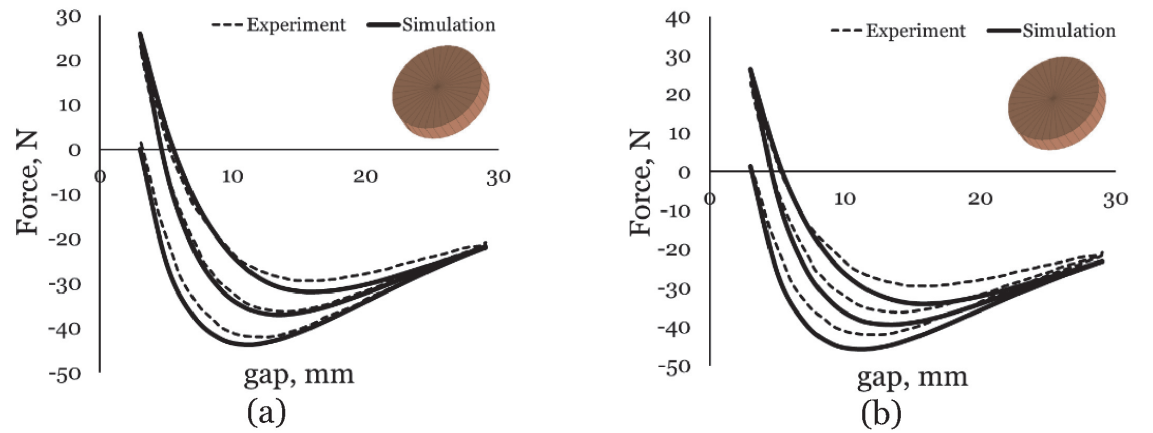*Force of HTS ring for ZFC: (a) model for current and (b) combined model.*

Figure 18.
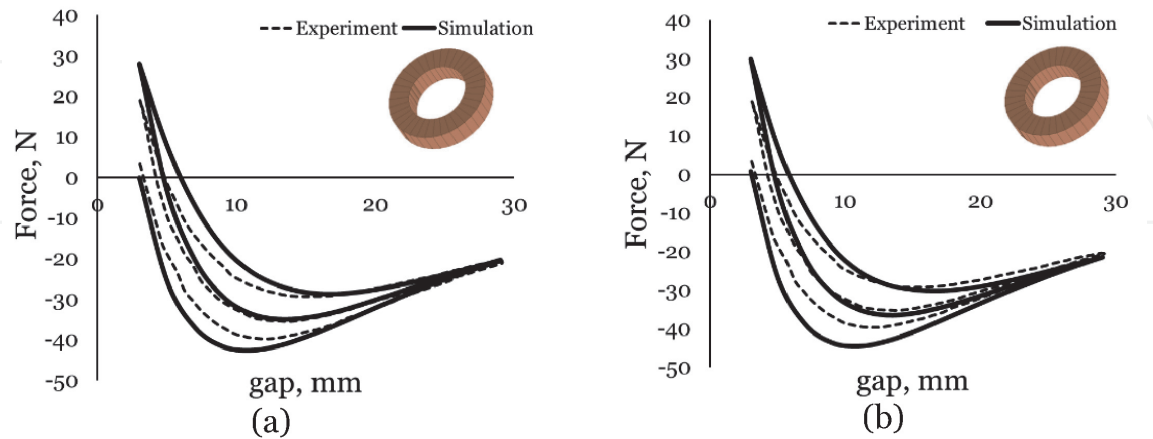*Force of HTS disk for FC: (a) model for current and (b) combined model.*

Figure 19.
Force of HTS ring for FC: (a) model for current and (b) combined model.

The difficulty lies in need to choose parameters that show a good approximation for both cooling modes – ZFC and FC.

The parameters selected based on the comparison with the measured results are presented in **Table 3**. Due to experimental confirmation, they can be considered as parameters of the studied HTS samples, and when studying several samples made of

Parameter	Units	Value
Critical current density, $J_{C,\mathrm{max}}$	A/mm^2	150
Critical magnetic field for current, H_C	kA/m	1100
α for critical current	—	1
β for critical current	—	2
Dispersion δ	—	0.003
Critical magnetization, $M_{C,\mathrm{max}}$	kA/m	80
Critical magnetic field for magnetization, H_{CM}	kA/m	1100
α for magnetization	—	1
β for magnetization	—	2

Table 3.
Parameters of the mathematical models for J and M from comparison with the experiment.

one material, as a characteristic of this material. Such a characteristic can be used in the design of devices based on bulk HTS with arbitrary sizes and shapes. To get closer to defining the parameters for material, rather than parameters for sample, two samples of different shapes were studied. Obtained parameters are suitable for both samples in both cooling modes.

During calculations and choosing of the model parameters, we assumed that both HTS samples have identical properties. However, the analysis of the experimental results of the experiment indirectly suggests some differences. The discrepancy between the calculated and experimental data was also influenced by inaccuracies of the experiment, in particular, some changes in the magnetization of the permanent magnet due to cooling by nitrogen at a minimum gap.

For illustrating the magnetization impact, all experimental dependencies were calculated for two models: model for current and combined model. At ZFC, magnetization causes the increase of the force at the minimal gap. At FC, magnetization shows the initial force at the cooling point, which is provided by the Meissner effect. In general, both models show good approximation with the experiment and can be recommended for analysis of magnetic systems with HTS bulk. As for magnetization, it should be applied in the system with a low gap, where it signally affects the characteristics of the system (force or trapped magnetic field), especially for FC.

Defined parameters, and the method for their determination, have limitations. Since they were selected and confirmed using experimental results at certain magnetic field range, their use is reliable only within the same field values.

6. Conclusion

The chapter discusses the methodology for modeling the electromagnetic properties of bulk HTS designed for the numerical calculation of magnetic systems. The proposed method is based on applying the two types of sources – current field and magnetization. The current properties are determined by nonlinear resistance. Magnetization is a model of local currents that can occur in a material, for example, upon transition into superconducting state. These currents do not obey the law of electromagnetic induction (in modeling). Their distribution in the volume can be represented as a characteristic of nonlinear magnetization.

Using the proposed models, we simulated the interaction of HTS bulk with external magnetic field after zero-field and field cooling. Distribution of the magnetic field sources inside a superconductor and magnetic field strength near it were obtained and analyzed. As shown in simulation results, the combination of two sources allows to widely regulate the properties of HTS and expand the possibilities of conventional methods, including the modeling of the Meissner effect.

For verification of the proposed method, we compare the results of simulation with the experimental measurements of the levitation force. Comparison shows the good agreement between calculated and measured results, which confirms the possibility to expand and clarify the approximation models describing the electromagnetic properties of bulk high-temperature superconductor.

Author details

Ekaterina Kurbatova[1*], Pavel Kurbatov[1] and Mikhail Sysoev[2]

1 National Research University "Moscow Power Engineering Institute", Moscow, Russia

2 Bauman Moscow State Technical University (National Research University), Moscow, Russia

*Address all correspondence to: kurbatovaep@mail.ru

IntechOpen

References

[1] Werfel FN, Floegel-Delor U, Rothfeld R, Riedel T, Goebel B, Wippich D, et al. Superconductor bearings, flywheels and transportation. Superconductor Science and Technology. 2012;**25**:014007. DOI: 10.1088/0953-2048/25/1/014007

[2] Krabbes G, Fuchs G, Canders WR, May H, Palka R. High Temperature Superconductor Bulk Materials: Fundamentals - Processing - Properties Control - Application Aspects. Wiley: Weinheim; 2006. p. 311. DOI: 10.1002/3527608044

[3] Coombs T. Bulk high temperature superconductor (HTS) materials. In: Melhem Z, editor. High Temperature Superconductors (HTS) for Energy Applications. Cambridge: Woodhead Publishing; 2012. pp. 101-139

[4] Kurbatova E. Comparative analysis of the specific characteristics of the magnetic bearings with HTS elements. IEEE Transactions on Applied Superconductivity. 2018;**28**:5207704. DOI: 10.1109/TASC.2018.2824347

[5] Naseh M, Heydari H. Analytical method for levitation force calculation of radial HTS magnetic bearings. IET Electric Power Applications. 2017;**11**: 369-377. DOI: 10.1049/iet-epa.2016.0070

[6] Kim SB, Ikegami T, Fujii Y, Takahashi M, Onodera H. Development of the noncontact rotating system using combined ring-shaped HTS bulks and permanent magnets. IEEE Transactions on Applied Superconductivity. 2014;**24**: 6800105. DOI: 10.1109/TASC.2013.2284021

[7] Arsenio AJ, Roque M, Cardeira C, Costa Branco PJ, Melicio R. Prototype of a zero-field-cooled YBCO bearing with continuous ring permanent magnets. IEEE Transactions on Applied Superconductivity. 2018;**28**:5207407. DOI: 10.1109/tasc.2018.2817279

[8] Mukoyama S et al. Development of superconducting magnetic bearing for 300 kW flywheel energy storage system. IEEE Transactions on Applied Superconductivity. 2017;**27**:3600804. DOI: 10.1109/ TASC.2017.2652327

[9] Wang J, Wang S. High Temperature Superconducting Magnetic Levitation. Berlin, Boston: De Gruyter; 2017. p. 388. DOI: 10.1515/9783110538434

[10] Floegel-Delor U, Schirrmeister P, Riedel T, Koenig R, Kantarba V, Werfel FN. Bulk superconductor levitation devices: Advances in and prospects for development. IEEE Transactions on Applied Superconductivity. 2018;**28**:3601605. DOI: 10.1109/tasc.2018.2809467

[11] Sotelo G, Dias D, Andrade R, Stephan R. Tests on a superconductor linear magnetic bearing of a full-scale MagLev vehicle. IEEE Transactions on Applied Superconductivity. 2011;**21**: 1464-1468. DOI: 10.1109/ TASC.2010.2086034

[12] Kurbatov P, Kurbatova E, Dergachev P, Kulayev Y. Simulation of the body motion in a tube with the linear HTS suspension. In: 2018 IEEE 18th International Power Electronics and Motion Control Conference (PEMC-2018); 26–30 August 2018; Budapest, Hungary. New York: IEEE; 2018. pp. 611-616. DOI: 10.1109/ EPEPEMC.2018.8521935

[13] Kovalev K, Koneev S, Poltavec V, Gawalek W. Magnetically levitated high-speed carriages on the basis of bulk HTS elements. In: Proceedings of 8th International Symposium on Maglev Suspension Technology (ISMST'8), 26–28 September 2005; Dresden, Germany. 2005. p. 51

[14] Deng Z et al. A high-temperature superconducting Maglev ring test line developed in Chengdu, China. IEEE Transactions on Applied Superconductivity. 2016;**26**:3602408. DOI: 10.1109/TASC.2016.2555921

[15] Bean C. Magnetization of high-field superconductors. Reviews of Modern Physics. 1964;**36**:31-39. DOI: 10.1103/RevModPhys.36.31

[16] Kim Y, Heampstead C, Strnad A. Critical persistent currents in hard superconductors. Physical Review Letters. 1962;**9**:306-309. DOI: 10.1103/PhysRevLett.9.306

[17] Ruiz-Alonso D, Coombs T, Campbell A. Numerical analysis of high-temperature superconductors with the critical state model. IEEE Transactions on Applied Superconductivity. 2004;**14**: 2053-2063. DOI: 10.1109/TASC.2004.838316

[18] Chun Y et al. Finite element analysis of magnetic field in high temperature bulk superconductor. IEEE Transactions on Applied Superconductivity. 2001;**11**: 2000-2003. DOI: 10.1109/77.920246

[19] Bean C. Response of high temperature superconductors to a step in magnetic field. In: Superconductivity and Applications (Proceedings of the Third Annual Conference on Superconductivity and Applications): 19–21 September 1989; New York. New York: Springer Science; 1989. pp. 767-772

[20] Sinder M, Meerovich V, Sokolovsky V, Vajda I. Penetration of magnetic field into high-temperature superconductors. IEEE Transactions on Applied Superconductivity. 1999;**9**: 4661-4665. DOI: 10.1109/77.819335

[21] Kim Y, Hempstead C, Strand A. Flux-flow resistance in type-II superconductors. Physical Review. 1965; **139**:A1163-A1172. DOI: 10.1103/PhysRev.139.A1163

[22] Vinen W, Warren A. Flux flow resistivity in type I superconductors: II. Theoretical discussion. Proceedings of the Physical Society. 1967;**91**:409-421. DOI: 10.1088/0370-1328/91/2/319

[23] Prigozhin L. Analysis of critical-state problems in type-II superconductivity. IEEE Transactions on Applied Superconductivity. 1997;**7**: 3866-3873. DOI: 10.1109/77.659440

[24] Rhyner J. Magnetic properties and AC-losses of superconductors with power-law current-voltage characteristics. Physica C. 1993;**212**: 292-300. DOI: 10.1016/0921-4534(93)90592-E

[25] Zou S, Zermeño V, Grilli F. Influence of parameters on the simulation of HTS bulks magnetized by pulsed field magnetization. IEEE Transactions on Applied Superconductivity. 2016;**26**:4702405. DOI: 10.1109/TASC.2016.2535379

[26] Douine B, Bonnard C, Sirois F, Berger K, Kameni A, Lévêque J. Determination of J_C and n-value of HTS pellets by measurement and simulation of magnetic field penetration. IEEE Transactions on Applied Superconductivity. 2015;**25**:8001008. DOI: 10.1109/TASC.2015.2409201

[27] Yokono T, Hasegawa K, Kamitani A. Magnetic shielding analysis of high-Tc superconducting plates by power law, flux-flow, and flux-creep models. IEEE Transactions on Applied Superconductivity. 2003;**13**:1672-1675. DOI: 10.1109/TASC.2003.812860

[28] Ikuno S, Kamitani A. Shielding current density analysis of axisymmetric HTS by element-free galerkin method. IEEE Transactions on Applied Superconductivity. 2005;**15**:3688-3691. DOI: 10.1109/TASC.2005.849393

[29] Anderson P. Theory of flux creep in hard superconductors. Physical Review Letters. 1962;**9**:309-311. DOI: 10.1103/PhysRevLett.9.309

[30] Klimenko E, Imenitov A, Shavkin S, Volkov P. Resistance–current curves of high pinning superconductors. Journal of Experimental and Theoretical Physics. 2005;**100**:50-65. DOI: 10.1134/1.1866198

[31] Kulaev Y et al. Modeling of electrophysical properties of bulk high-temperature superconductors in calculations of magnetic systems. Russian Electrical Engineering. 2015;**86**: 213-219. DOI: 10.3103/S10683712150 40070

[32] Stratton J. Electromagnetic Theory. New York: McGraw-Hill; 1941. p. 631

[33] Kulaev Y, Kurbatov P, Kurbatova E. Construction of combined models of the properties of bulk high-temperature superconducting materials. Russian Electrical Engineering. 2017;**88**:465-470. DOI: 10.3103/s1068371217070094